
1 **Frequent haze events associated with transport and stagnation over**
2 **the corridor between [the](#) North China Plain and Yangtze River Delta**

3 Feifan Yan¹, Hang Su², Yafang Cheng², Rujin Huang³, Hong Liao⁴, Ting Yang⁵,
4 Yuanyuan Zhu⁶, Shaoqing Zhang⁷, Lifang Sheng⁸, Wenbing Kou¹, Xinran Zeng⁹,
5 Shengnan Xiang¹, Xiaohong Yao¹, Huiwang Gao¹, Yang Gao^{1*}

6 ¹Frontiers Science Center for Deep Ocean Multispheres and Earth System (FDOMES) and Key
7 Laboratory of Marine Environmental Science and Ecology, Ministry of Education, Ocean
8 University of China, and Laoshan Laboratory, Qingdao, 266100, China

9 ²Max Planck Institute for Chemistry, Multiphase Chemistry Department, Mainz D-55128, Germany

10 ³State Key Laboratory of Loess and Quaternary Geology (SKLLQG), Center for Excellence in
11 Quaternary Science and Global Change, Institute of Earth Environment, Chinese Academy of
12 Sciences, Xi'an 710061, China

13 ⁴Jiangsu Key Laboratory of Atmospheric Environment Monitoring and Pollution Control, Jiangsu
14 Engineering Technology Research Center of Environmental Cleaning Materials, Collaborative
15 Innovation Center of Atmospheric Environment and Equipment Technology, School of
16 Environmental Science and Engineering, Nanjing University of Information Science &
17 Technology, Nanjing 210044, China

18 ⁵State Key Laboratory of Atmospheric Boundary Layer Physics and Atmospheric Chemistry,
19 Institute of Atmospheric Physics, Chinese Academy of Sciences, Beijing, 100029, China

20 ⁶China National Environmental Monitoring Centre, Beijing 100012, China

21 ⁷Frontiers Science Center for Deep Ocean Multispheres and Earth System, and Key Laboratory of
22 Physical Oceanography, Ministry of Education, the College of Oceanic and Atmospheric Sciences,
23 Ocean University of China, and Laoshan Laboratory, Qingdao, 266100, China

24 ⁸College of Oceanic and Atmospheric Sciences, Ocean University of China, Qingdao, 266100,
25 China

26 ⁹Zhejiang Institute of Meteorological Sciences, Hangzhou, 310008, China

27
28 *Correspondence to: yanggao@ouc.edu.cn

Abstract

PM_{2.5} pollution is a major air quality issue ~~deterioratingthat~~ deteriorates human health, and numerous studies ~~feeshave~~ focused on PM_{2.5} pollution in major regions such as the North China Plain (NCP) and Yangtze River Delta (YRD). However, the characteristics of PM_{2.5} concentrations and the associated formation mechanism in the transport corridor (referred to as SWLY) between the NCP and YRD are largely ignored. Based on observational data, we find that the number of PM_{2.5} pollution events in SWLY is comparable to that in NCP, far exceeding ~~thosethat~~ in YRD, which is indicative of the severity of air pollution ~~everin~~ this area. Utilizing a regional climate and air quality model, we isolate the effect of seesaw transport events, e.g., transport between the NCP and YRD, as well as ~~the~~ atmospheric stagnation on the accumulation of PM_{2.5} over SWLY. Specifically, seesaw events and stagnation, comparable to each other, collectively account for an average of 67% of pollution days with PM_{2.5} exceeding 75 µg/m³, and this fraction (85%) is even larger for severe haze events with PM_{2.5} exceeding 150 µg/m³. Furthermore, the connection between seesaw transport and large-scale circulation is examined. The ~~trans-regional~~transregional transport of pollutants from the NCP to the YRD (YRD to NCP) is likely stimulated by positive (negative) to negative (positive) geopotential height ~~anomaly~~anomalies at 500 hPa located in northern China. The health effect due to short-term PM_{2.5} exposure induced by the ~~trans-regional~~transregional transport and stagnation is investigated, yielding a total of 8,634 (95% CI: 6,023-11,223) and 9,496 (95% CI: 6,552-12,413) premature deaths, respectively, in SWLY during winter 2014-2019, which is as high as 9% of the total premature deaths in China ~~although, even though~~ the ~~area coverage of~~ SWLY is ~~withintakes up less than~~ 1%.% of China's area. While atmospheric stagnation is in ~~general~~generally projected to occur more frequently under a warming climate, this study indicates the importance of regional emission control to alleviate PM_{2.5} pollution from seesaw transport and stagnation.

61

62

63 **1 Introduction**

64 With the rapid development of the economy, particulate matter with diameters less
65 than 2.5 μm ($\text{PM}_{2.5}$) has become a major issue ~~deteriorating~~deteriorates air quality in
66 China and ~~threatening~~threatens human health, e.g., causing serious respiratory, and
67 cardiovascular diseases and even premature death (~~Donaldson et al., 1998; Pui et al.,~~
68 ~~2014; Xing et al., 2016~~)(Donaldson et al., 1998; Pui et al., 2014; Xing et al., 2016).
69 Strict emission control strategies have been carried out since the severe haze pollution
70 events in 2013, leading to a generally decreasing trend of annual mean $\text{PM}_{2.5}$
71 concentrations (~~Zhang et al., 2019b~~)(Zhang et al., 2019b). Nevertheless, ~~besides~~in
72 ~~addition to~~ emissions, unfavorable meteorological conditions, such as atmospheric
73 stagnation (~~Gao et al., 2020; Wang et al., 2022~~)(Gao et al., 2020; Wang et al., 2022) and
74 ~~trans-regional~~transregional transport of air pollutants (~~Huang et al., 2020; Kang et al.,~~
75 ~~2021; Ma et al., 2017~~)(Huang et al., 2020; Kang et al., 2021; Ma et al., 2017),
76 ~~remain~~continue to stimulate the accumulation of local $\text{PM}_{2.5}$, ~~which is~~ conducive to
77 ~~exceedance of~~creating air pollution at levels that exceed the Chinese Ambient Air
78 Quality Standards.

79 In China, severe $\text{PM}_{2.5}$ pollution in eastern China has received ~~a lot of~~much
80 attention, especially in ~~the~~ North China Plain (NCP) (~~Wang et al., 2014; Zhang et al.,~~
81 ~~2015~~)(Wang et al., 2014; Zhang et al., 2015) and the Yangtze River Delta (YRD) (~~Jia~~
82 ~~et al., 2022; Li et al., 2019a~~)(Jia et al., 2022; Li et al., 2019a). Several studies ~~pointed~~
83 ~~out~~have noted that air pollutants can be transported between ~~the~~ NCP and YRD (~~He et~~
84 ~~al., 2018; Huang et al., 2020; Kang et al., 2019; Zhang et al., 2021a~~)(He et al., 2018;
85 ~~Huang et al., 2020; Kang et al., 2019; Zhang et al., 2021a~~). For instance, by applying
86 the source apportionment method, ~~Kang et al. (2019)~~Kang et al. (2019) found that ~~the~~
87 transport due to cold frontal ~~passage~~passages from ~~the~~ NCP contributed to 29% of ~~the~~
88 severe $\text{PM}_{2.5}$ pollution, with $\text{PM}_{2.5}$ concentrations as high as $300 \mu\text{g m}^{-3}$ during 21–26
89 January 2015 in ~~the~~ YRD. Similarly, ~~Huang et al. (2020)~~Huang et al. (2020) found that

90 ~~the~~ air ~~pollutant~~pollutants from ~~the~~ YRD could ~~transport~~be transported to ~~the~~ NCP,
91 lowering the planetary boundary layer height (PBLH) through ~~the~~ aerosol direct
92 radiative effect and ~~aggravate~~aggravating the accumulation of PM_{2.5} concentrations
93 therein, which can then be transported back to ~~the~~ YRD by cold fronts. In fact, the
94 region located in the connecting belt of these two areas, particularly at the junction of
95 four provinces (Jiangsu, Anhui, Shandong, Henan))₂ referred to as SWLY, experiences
96 heavy PM_{2.5} pollution in China (~~Wu et al., 2018; Xie et al., 2016~~)(Wu et al., 2018; Xie
97 et al., 2016). Moreover, high PM_{2.5} concentrations pose a remarkable health risk due to
98 the dense population in SWLY (~~Li et al., 2019b; Yang et al., 2018~~)(Li et al., 2019b;
99 Yang et al., 2018). Nevertheless, there are very limited studies investigating the
100 transport effects on PM_{2.5} concentrations in SWLY.

101 ~~Besides~~In addition to the transport, atmospheric stagnation plays an essential role
102 in magnifying local air pollution in China. Previous studies indicated that atmospheric
103 stagnation exhibited a high spatial correlation with PM_{2.5} pollution over eastern China
104 (~~Wang et al., 2022~~)(Wang et al., 2022) and favored the accumulation in PM_{2.5}
105 concentrations (~~Gao et al., 2020; Wang et al., 2018b~~)(Gao et al., 2020; Wang et al.,
106 2018b). For instance, ~~Wang et al. (2022)~~Wang et al. (2022) found that more than two
107 thirds of stagnant days could lead to high PM_{2.5} concentrations exceeding the 90th
108 percentile in ~~the~~ NCP during 2013-2018. During 1985-2014, the most evident
109 increasing trend of atmospheric stagnation frequency was found in the eastern flank of
110 China, including the SWLY region (~~Huang et al., 2017~~)(Huang et al., 2017), and how
111 these weather conditions induce PM_{2.5} pollution ~~over there~~remains unclear.

112 PM_{2.5} exerts substantial health effects, among which ~~the~~ long-term exposure effect
113 has been widely acknowledged (~~REF~~)(Ali et al., 2023; Geng et al., 2021), and recent
114 studies ~~have~~ indicated striking health burdens resulting from short-term exposure to
115 PM_{2.5} as well (~~Jiang et al., 2020; Li et al., 2019b; Liu et al., 2021~~)(Jiang et al., 2020; Li
116 et al., 2019b; Liu et al., 2021). ~~For example, Li et al. (2019b).~~ For example, Li et al.
117 (2019b) found 169,862 additional deaths attributed to short-term PM_{2.5} exposure in
118 China in 2015, with the highest death rate of 14.63 (95%CI: 8.50-20.69) per 100,000

119 ~~people in the eastern China. Liu et al. (2021) CI: 8.50-20.69 per 100,000 people in~~
120 ~~eastern China. Liu et al. (2021)~~ found that Shandong, Jiangsu, Hebei, and Henan
121 experienced the highest health ~~costs~~ (medical cost, productivity loss, etc.) in China
122 attributable to short-term PM_{2.5} pollution during 2013-2018. Therefore, it is of great
123 importance to investigate the health burdens associated with short-term exposure to
124 PM_{2.5} concentrations, as well as the contributions resulting from different
125 meteorological conditions, e.g., ~~trans-regional~~transregional transport and stagnant
126 weather in SWLY.

127 To this end, we conduct ~~the~~ numerical simulations with Weather Research and
128 Forecasting (WRF) and Community Multiscale Air Quality (CMAQ) from 2014 to
129 2019, aiming to isolate the effects of transport (~~section~~Section 3.2) and atmospheric
130 stagnation (~~section~~Section 3.3) on PM_{2.5} in SWLY. ~~At the end~~Finally, the health impact
131 of PM_{2.5} caused by ~~trans-regional~~transregional transport and stagnation is quantified.

132

133 **2 Model configuration and methods**

134 **2.1 Model configuration**

135 This study applies WRF version 4.1.1 and CMAQ version 5.3.1 to simulate the
136 meteorological and air quality conditions from 2014 to 2019. The simulation domain is
137 shown in Fig. S1, and the spatial resolution is 36 km × 36 km. There are 34 vertical
138 layers from ~~the~~ surface to 50 hPa with denser layers within the planetary boundary layer
139 (PBL) to better reproduce the air pollutant concentrations within the layer (~~Appel et al.,~~
140 ~~2007; Wang et al., 2011~~)(Appel et al., 2007; Wang et al., 2011). The physics schemes
141 in WRF are shown in Table S1, ~~and are~~ consistent with ~~the~~ previous study (~~Zeng et al.,~~
142 ~~2022~~)(Zeng et al., 2022). The NCEP Climate Forecast System Reanalysis (CFSR)
143 version 2 (~~Saha et al., 2014~~)(Saha et al., 2014), with horizontal resolutions of 0.5° ×
144 0.5°, provides the initial and boundary conditions for WRF simulations. To improve the
145 meteorological simulations to enhance the simulation capability of air quality model,
146 gird nudging technique is applied (Bowden et al., 2012; Liu et al., 2012). Only U and
147 V nudging above the boundary layer was applied, with a nudging coefficient of 3*10⁻⁴.

域代码已更改

148 The gas chemical mechanism of Carbon-Bond version 6 (CB6) (~~Luecken et al.,~~
149 ~~2019~~)(Luecken et al., 2019) and the aerosol module of AERO7 are used (~~Appel et al.,~~
150 ~~2021; Pye et al., 2017~~)(Appel et al., 2021; Pye et al., 2017). The chemical initial and
151 boundary conditions of CMAQ are downscaled from the Model for Ozone and Related
152 chemical Tracers, version 4 (MOZART-4) (~~Emmons et al., 2010~~)(Emmons et al., 2010),
153 the same method as applied in Ma et al. (2019).

154 In this study, ~~the~~ anthropogenic emissions inventory in ~~the year of~~ 2016 is derived
155 from the Multi-resolution Emission Inventory for China version 1.2 (MEIC v1.2;
156 <http://www.meicmodel.org> (~~Li et al., 2017; Zheng et al., 2018~~)(Li et al., 2017; Zheng
157 ~~et al., 2018~~)), which mainly includes emissions from agriculture, ~~resident~~residents,
158 transportation, industry and power plants. The ship emissions are from ~~Shipping~~the
159 ~~shipping~~ emission inventory model (SEIM) (~~Liu et al., 2016; Liu et al., 2019b~~)(Liu et
160 ~~al., 2016; Liu et al., 2019b~~). The biomass burning emission inventory from 2014-2019
161 is based on Global Emission Database ~~version 4~~version 4.1 (GFEDv4.1; (~~Giglio et al.,~~
162 ~~2013; Van der Werf et al., 2017~~)(Giglio et al., 2013; Van der Werf et al., 2017)). The
163 hourly biogenic emissions are generated by ~~the~~ Model of Emission of Gases and
164 Aerosol from Nature (MEGAN) (~~Guenther et al., 2012~~)(Guenther et al., 2012). For the
165 evaluation of model simulations, the meteorological observation data ~~is~~are available at
166 the National Climatic Data Center (NCDC, [https://www.ncdc.noaa.gov/data-](https://www.ncdc.noaa.gov/data-access/quick-links#dsi-3505)
167 [access/quick-links#dsi-3505](https://www.ncdc.noaa.gov/data-access/quick-links#dsi-3505); last access: December 8, 2021), including air temperature
168 at 2 m, wind speed and direction at 10 m. The observational hourly PM_{2.5} data are taken
169 from the China National Environmental Monitoring Centre (<http://www.pm25.in>, last
170 access: September 23, 2021). In this study, the ~~simulation time for WRF and CMAQ is~~
171 ~~six full years from 2014 to 2019. The simulations are conducted continuously for each~~
172 ~~year, with December in the previous year as the spin-up time. To facilitate the analysis,~~
173 ~~the three months (of January, February, and December) of each in the same year, are~~
174 referred to as the ~~winter~~ season ~~of winter, is focused considering it is the major haze~~
175 ~~period.~~

176 2.2 Short-term exposure premature death to PM_{2.5}

In order to quantify the health effects attributable to exposure to PM_{2.5}, we calculate all-cause premature deaths associated with the short-term exposure to PM_{2.5} during 2014-2019. The following formula is used as shown below:

$$RR_{i,j} = \exp[\beta \times \max(C_{i,j} - C_0, 0)]$$

$RR_{i,j}$ represents the relative risk for deaths from all-cause causes, where i and j represent the day and grid, respectively. $C_{i,j}$ is the daily average concentration of PM_{2.5}. For the days with a mean PM_{2.5} greater than or equal to 75 $\mu\text{g m}^{-3}$, C_0 equals to 75 $\mu\text{g m}^{-3}$, and the exposure-response coefficient β is set to be 1.22% (95% CI: 0.82–1.63%) per 10 $\mu\text{g m}^{-3}$ increase of PM_{2.5} (Sun et al., 2022)(Sun et al., 2022). For all the other days which that are considered relatively clean, C_0 equals to zero, β is set to be 0.41% (95% CI: 0.32–0.50%) per 10 $\mu\text{g m}^{-3}$ increase of PM_{2.5} (Liu et al., 2019a)(Liu et al., 2019a). The age structure is not considered in this formula because of little significant differences in mortality among age subgroups (Sun et al., 2022)(Sun et al., 2022).

$$\text{Death}_{i,j} = Y_{i,j} \times P_j \times (1 - 1/RR_{i,j})$$

$\text{Death}_{i,j}$ represents the number of premature deaths at a specific grid on a day; $Y_{i,j}$ is the daily baseline mortality rate, which is obtained from the Global Burden of Disease (GBD) 2019 data (<https://vizhub.healthdata.org/gbd-results/>; (Berman et al., 2020)(Berman et al., 2020)). P_j represents the number of populations.

2.3 Definition of seesaw events and air stagnation

In this study, we focus on two meteorological scenarios during wintertime in 2014-2019: seesaw events and air stagnation. The seesaw events are diagnosed as follows: over a three-day period, the mean PM_{2.5} concentration over the NCP (YRD) decreases by more than a certain threshold whereas it increases continuously during the period over the YRD (NCP), leading to two types of seesaw events. In this study, we select a threshold of 40%, which identified a total of 168 days with the seesaw pattern. Additionally, we test several other thresholds (e.g., 30%, 35%, 45%, 50%), which resulted in comparable numbers of seesaw pattern days: 182, 176, 162, and 154,

带格式的: 字体: 加粗

带格式的: 缩进: 首行缩进: 0 字符

205 respectively. Regarding air stagnation, we adopted the criteria proposed by [Gao et al.](#)
206 [\(2020\)](#)[Gao et al. \(2020\)](#). A stagnant day is defined as a day where the daily mean wind
207 speed at 10 m is less than 3.2 m/s, the daily total precipitation is less than 1 mm and the
208 planetary boundary layer height is less than 520 m.

209 Please note that there is an overlap between stagnant and seesaw events. Among
210 the seesaw events, 35% are concomitant with stagnant conditions, indicating that the
211 seesaw events together with stagnant weather conditions are more conducive to high
212 PM_{2.5} pollution. As a result, when discussing the seesaw pattern, the concomitant
213 stagnant days are included.

214 **3 Results and ~~discussions~~discussion**

215 **3.1 Model validation**

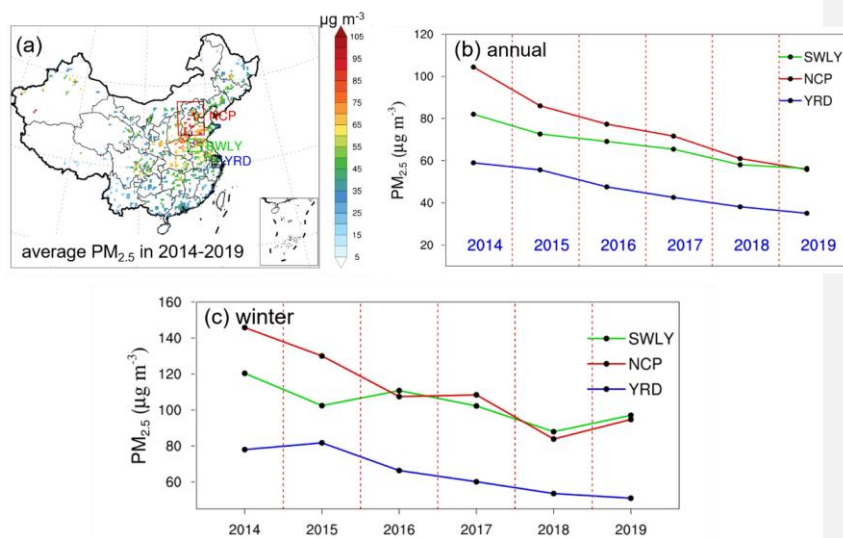
216 To evaluate the capability of [the model](#) ~~in reproducing~~ [to reproduce](#) the
217 observations, we first compared the meteorological parameters, including daily air
218 temperature at 2 m (T2), specific humidity at 2 m (Q2), wind speed at 10 m (WS10)
219 and wind direction at 10 m (WD10), simulated by WRF (Table S2) against the
220 observations of the NCDC over [the](#) NCP, YRD, and SWLY. The statistical metrics,
221 including mean bias, gross error, and root-mean-square error (RMSE), are mostly
222 within the benchmarks [\(Emery and Tai, 2001\)](#)[\(Emery and Tai, 2001\)](#), despite the
223 slightly higher bias for wind direction which is likely attributable to wind directions
224 close to 0° or 360° [\(Zhang et al., 2019a\)](#)[\(Zhang et al., 2019a\)](#). Moreover, daily mean
225 simulated PM_{2.5} is compared to observations during 2014-2019 over the three regions
226 of NCP, YRD, and SWLY (Fig. S2). Overall, the mean fractional bias (MFB) and mean
227 fractional error percent (MFE) are within the benchmarks (MFB ≤ ±50%, MFE ≤ 75%,
228 US [EPA \(2007\)](#)[EPA \(2007\)](#)), warranting ~~a~~ high confidence ~~of~~ [in](#) interpreting the
229 simulated results.
230

231 **3.2 Observational evidence of high PM_{2.5} concentrations in SWLY**

232 Figure 1a shows the spatial distribution of observed mean PM_{2.5} concentrations
233

234 from 2014 to 2019. The high values of $PM_{2.5}$ are predominantly
 235 concentrated in eastern China due to dense populations and anthropogenic
 236 emissions (Gao et al., 2022)(Gao et al., 2022). Zooming into the SWLY, NCP and YRD,
 237 the annual mean $PM_{2.5}$ in these three regions gradually decreases, primarily attributable
 238 to strict clean air policies and reductions in anthropogenic emissions (Zhang et al.,
 239 2019b)(Zhang et al., 2019b). Among the three regions, the average $PM_{2.5}$ concentration
 240 is highest in the NCP ($76.0 \mu g m^{-3}$), followed closely by the SWLY with a $PM_{2.5}$
 241 concentration of $67.2 \mu g m^{-3}$, which is much higher than that over the
 242 YRD ($46.3 \mu g m^{-3}$). Furthermore, as shown in Fig. 1b, despite the adjacency of the
 243 SWLY to NCP, the decreasing trend is more pronounced in NCP ($9.3 \mu g m^{-3} a^{-1}$),
 244 followed by YRD ($5.1 \mu g m^{-3} a^{-1}$) and SWLY ($5.0 \mu g m^{-3} a^{-1}$). When focusing
 245 specifically on the winter season, as shown in Fig. 1c, $PM_{2.5}$ concentrations in NCP and
 246 SWLY are almost comparable from 2016 to 2019 and much higher than in YRD,
 247 indicating a more severe haze pollution situation in winter in SWLY compared to YRD.
 248 Note that the line separation between NCP and SWLY in the winter of 2014 and 2015
 249 will be discussed in the subsequent paragraph.

250



251

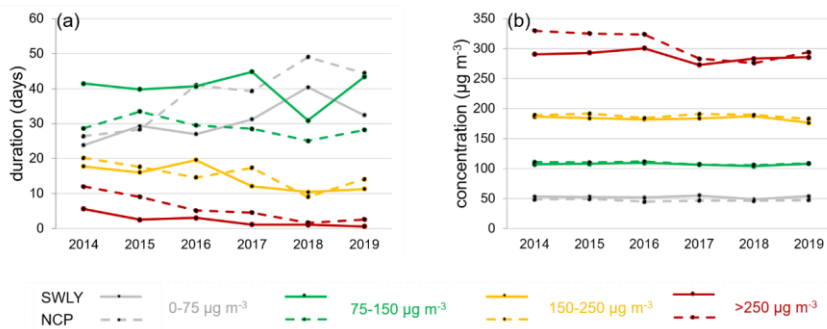
252 Figure 1. a: Spatial distribution of six-year annual mean $PM_{2.5}$. b,c: Time series of

253 annual (b) and winter (c) mean PM_{2.5} concentrations over ~~the~~ SWLY, NCP, and YRD
254 regions.

255
256 According to the Air Quality Index (HJ 633-2012; ~~(MEEPRC, 2012)~~~~(MEEPRC,~~
257 ~~2012)~~), a pollution day is defined as a day with ~~a~~ mean PM_{2.5} concentration exceeding
258 75 µg m⁻³, which can be further divided into moderate pollution (75-150 µg m⁻³), heavy
259 pollution (150-250 µg m⁻³) and extreme pollution (greater than 250 µg m⁻³). To better
260 measure the severity of pollution, a metric of duration is ~~indeed introduced~~, which is
261 calculated as the regional mean value of ~~the~~ total number of pollution days in winter.
262 The number of pollution days in one event is considered ~~as persistence~~~~persistent~~, and
263 we have also calculated the mean persistence of all events. Figure 2 shows the duration,
264 ~~as well as and~~ mean regional PM_{2.5} concentrations over SWLY and NCP during these
265 pollution days, for these three ~~categories~~~~abovementioned~~ ~~categories~~. Here, some
266 discussion is needed to show why we introduce these parameters, and which kind of
267 information it could bring us beyond a simple PM_{2.5} concentration.

268 During wintertime in 2014-2019, the total annual number of pollution days ~~reaches~~
269 ~~or reached an~~ average of 57.1 and 50.3 in SWLY and NCP, respectively (Fig. 2a). By
270 classifying pollution days into different categories, the results depicted in Fig. 2b
271 indicate that ~~the~~ extreme pollution events, characterized by daily mean PM_{2.5}
272 concentrations exceeding 250 µg m⁻³, dominate the interannual variability ~~of in~~ winter
273 PM_{2.5} in both ~~the~~ SWLY and NCP (Fig. 1c). Similarly, as shown in Fig. ~~S4S3~~, in 2014
274 and 2015, the cumulative distribution function curves of daily ~~observational~~~~observed~~
275 PM_{2.5} in ~~the~~ NCP are obviously on the right of ~~that those~~ in ~~the~~ SWLY, indicating higher
276 PM_{2.5} concentrations over ~~the~~ NCP. Since 2016, the cumulative distribution function
277 curves over SWLY are on the right of ~~that those~~ in NCP when ~~the~~ PM_{2.5} concentration
278 is below 100-150 µg m⁻³, which reverses when ~~the~~ PM_{2.5} concentration becomes higher,
279 yielding an overall comparable PM_{2.5} concentration between NCP and SWLY. While
280 both SWLY and NCP experience comparably frequent PM_{2.5} pollution events, higher
281 than that over YRD (Fig. ~~S5a~~~~S4a~~), the higher total number of PM_{2.5} pollution days in

282 SWLY indicates that the meteorological features in SWLY may govern the severe
 283 pollution ~~over~~ there, considering that the mean precursor emissions (such as NO_x and
 284 SO₂) in SWLY are only 68% and 52% of those in the NCP (Fig. S6S5).
 285



286
 287 Figure 2. The regional mean number of days (duration) (a) and concentrations (b) of
 288 observational PM_{2.5} for the four categories (I: 0-75 µg m⁻³, II: 75-150 µg m⁻³, III: 150-
 289 250 µg m⁻³ and IV: greater than 250 µg m⁻³) over SWLY (solid lines) and NCP (dotted
 290 lines) in winter ~~from 2014 to 2019~~.
 291

292 3.3 The seesaw effect between NCP and YRD on PM_{2.5} in SWLY

293 Considering that SWLY is located in the corridor between ~~the~~ NCP and YRD, ~~the~~
 294 transport from ~~the~~ polluted ~~areareas~~ such as ~~the~~ NCP and YRD could play key roles ~~in~~
 295 affecting air quality in SWLY. To diagnose the effect, two types of seesaw events are
 296 defined in this study. Type I seesaw events are characterized by a decrease (40%
 297 threshold) in PM_{2.5} concentration over ~~the~~ NCP and an increase over ~~the~~ YRD, while
 298 Type II seesaw events show the opposite pattern.

299 The temporal evolution of mean composited PM_{2.5} concentrations during winter
 300 2014-2019 in SWLY, NCP and YRD for Type I and II seesaw events are shown in Fig.
 301 3a-b. For Type I events (Fig. 3a), there is a total of 24 events lasting 75 days, with ~~an~~
 302 ~~average~~ persistence ~~on average~~ of 3 days. On ~~dayDay~~ 1, the PM_{2.5} concentrations are
 303 highest over ~~the~~ NCP (144.5 µg m⁻³), followed by ~~the~~ SWLY (103.9 µg m⁻³) and YRD
 304 (32.1 µg m⁻³), ~~respectively~~. On ~~dayDay~~ 2, along with a sharp decrease in ~~the~~ PM_{2.5}

305 concentration in [the](#) NCP ($112.9 \mu\text{g m}^{-3}$), the $\text{PM}_{2.5}$ in SWLY rapidly ~~increases~~[increased](#)
306 by 31% ($135.2 \mu\text{g m}^{-3}$). Finally, on the third day, when $\text{PM}_{2.5}$ pollution is cleared out in
307 [the](#) NCP ($59.0 \mu\text{g m}^{-3}$), $\text{PM}_{2.5}$ concentrations in SWLY ~~remains to be~~[remain](#) as high as
308 $108.7 \mu\text{g m}^{-3}$ and ~~it increases~~[increase](#) to $94.3 \mu\text{g m}^{-3}$ in [the](#) YRD. Fig. 3c further denotes
309 wind vectors at 850 hPa which supports the movement of [the](#) surface $\text{PM}_{2.5}$
310 concentration. On ~~day~~[Day](#) 1, the weak wind over North China favors the accumulation
311 of $\text{PM}_{2.5}$ in [the](#) NCP, and the particulate ~~matters propagate~~[matter propagates](#)
312 southeastward, driven by the enhanced northwesterly wind, resulting in high $\text{PM}_{2.5}$
313 concentrations in SWLY and YRD on ~~day~~[Day](#) 2 and 3. Previous studies have pointed
314 out [that](#) the ~~trans-boundary~~[transboundary](#) effect from [the](#) NCP to [the](#) YRD contributed
315 to almost one-third of [the](#) total $\text{PM}_{2.5}$ in [the](#) YRD during ~~the~~ periods such as January
316 21-26, 2015 (~~Kang et al., 2019~~)[\(Kang et al., 2019\)](#) and November 2-3, 2017 (~~Kang et~~
317 ~~al., 2021~~)[\(Kang et al., 2021\)](#), respectively.

318
319 Similarly, in Type II events (Fig. 3b) during which $\text{PM}_{2.5}$ is transported from [the](#)
320 YRD toward [the](#) northwest ~~direction~~, there is a total of 106 days with 32 events.
321 Compared to ~~day~~[Day](#) 1, [the](#) $\text{PM}_{2.5}$ concentrations ~~in day~~[on Day](#) 3 over [the](#) YRD
322 ~~decreases~~[decrease](#) rapidly by 63%, while ~~it increases~~[they increase](#) by 82% over [the](#)
323 NCP ($111.7 \mu\text{g m}^{-3}$). Meanwhile, SWLY maintains a stable pollutant status, with $\text{PM}_{2.5}$
324 concentrations of $59.4\text{-}131.9 \mu\text{g m}^{-3}$. The spatiotemporal evolution of surface $\text{PM}_{2.5}$
325 concentrations and wind ~~vector~~[vectors](#) at 850 hPa during this event is displayed in Fig.
326 3d. Unlike Type I (Fig. 3c), on ~~day~~[Day](#) 1, strong northwesterly ~~wind~~[winds](#) in
327 ~~north~~[northern](#) China ~~is~~[are](#) concomitant with low $\text{PM}_{2.5}$ concentrations over NCP,
328 while the $\text{PM}_{2.5}$ [concentrations](#) in southern China, such as [the](#) YRD and ~~the~~-adjacent
329 areas, are relatively high. In the following two days, the northwesterly wind
330 ~~retreat~~[retreated](#) further north, and ~~a~~ weak southerly wind ~~dominates~~[dominated](#) the
331 majority of North China, stimulating the accumulation of $\text{PM}_{2.5}$ in [the](#) SWLY and NCP.
332 Comparably, focusing ~~an~~ episodic events ~~during~~[from](#) October 29 to November 6,
333 2015 over [the](#) NCP, ~~Zhang et al. (2021b)~~[Zhang et al. \(2021b\)](#) found that transport from

带格式的: 突出显示

the south could account for up to 70% of $PM_{2.5}$ concentrations over this area.

Moreover, the Lagrangian particle dispersion model FLEXPART working together with WRF (FLEXPART-WRF; (Brioude et al., 2013)) is applied to identify the dominant wind direction for each event in types I and II, with the target regions of YRD and NCP, respectively. A total of 72 hours, with an interval of 12 hours are backward tracked to identify the transport pathways, yielding a total of 7 trajectories marked in different colors for each event, as shown in Fig. S6-7. For type I, most seesaw events are driven by the northwesterly wind, leading to an increase in $PM_{2.5}$ concentrations in the SWLY and YRD regions. Even though there are a few exceptions, for instance, on February 2 and 27 2014, the wind direction 72 hours prior to the event may be quite different from the other two days (e.g., 24 hours and 48 hours), which in general favors the northwesterly transport, indicating that the wind pattern closer to the end of the event may play a larger role in fostering the accumulation of high $PM_{2.5}$ concentrations downwind of the pollution area. In contrast, for type II, the seesaw pattern of the $PM_{2.5}$ concentration in the NCP is attributed to the shift in the dominant wind direction, that is, from northwest to southwest (Fig. S7), which facilitates $PM_{2.5}$ accumulation over the NCP.

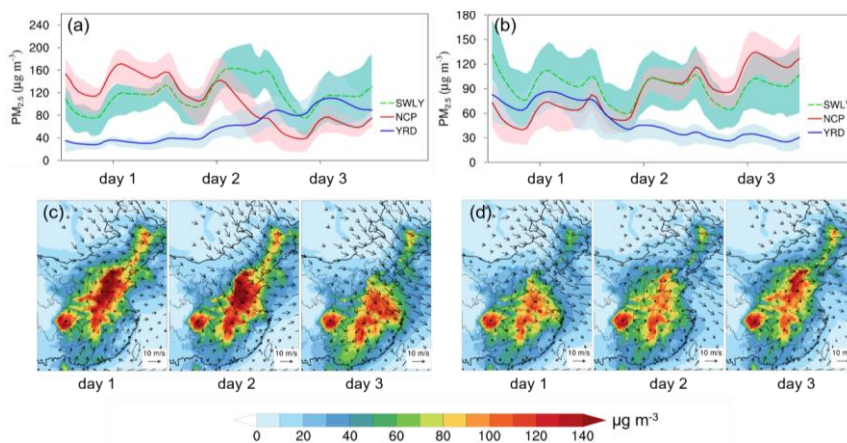
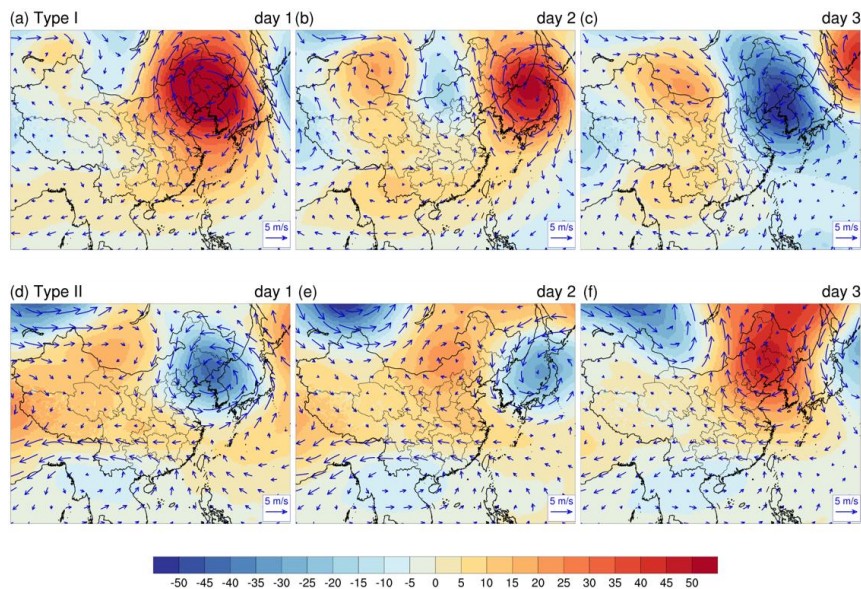


Figure 3. First row: Time series of mean $PM_{2.5}$ concentrations in the SWLY (green dashed line), NCP (red solid line) and YRD (blue solid line), with shading indicative of

355 the range of the 25th-75th percentile, during winter 2014-2019 for type I (a) and type II
356 (b). Second row: The spatial distribution shows the surface average PM_{2.5}
357 concentrations during three days in type I (c) and type II (d), respectively, with black
358 arrows representing the wind vectors at 850 hPa.

359
360 There is a tight relationship between the surface PM_{2.5} concentration and upper-
361 level large-scale circulations (e.g., 500 hPa) in eastern China (Hua and Wu, 2022;
362 Zhang et al., 2022)(Hua and Wu, 2022; Zhang et al., 2022). To this end, we composite
363 the anomalous 500 hPa geopotential height and wind vector during Type I and II events.
364 As shown in Fig. 4a, for Type I, the NCP is located westwardwest of the center of
365 intense anticyclonic anomalies—center, conducive to the accumulation of PM_{2.5}
366 concentrations therein throughby inducing relatively stagnant weather conditions
367 (Wang et al., 2020; Zhong et al., 2019)(Wang et al., 2020; Zhong et al., 2019). Based
368 on observations during 2009-2020 as mentioned in Hua and Wu (2022), theHua and
369 Wu (2022), negative-positive height anomalies could be regarded as a reliable signal
370 for wintertime haze occurrence in Beijing. On dayDay 2 and 3, the high-pressure system
371 center retreatretreated eastward, and—a triple feature emergesemerged, with a positive-
372 negative-positive pattern in northern of China from west to east, and the middle low-
373 pressure system favorsfavored the air transport from North—China—Plainthe NCP,
374 eventually formforming the high PM_{2.5} in the SWLY and YRD. In contrast, the spatial
375 evolution of the pressure system behaves oppositely for Type II events (Fig. 4b). The
376 North China is controlled by a low-pressure system on the—dayDay 1, supporting the
377 low PM_{2.5} over thereconcentration and relatively high PM_{2.5} concentration over the
378 YRD and southern China. Along with the movement of air flow, a high—pressure system
379 kicks in and takestakes over, facilitating the transport of moist and warm airflow and
380 subsequentlysubsequent secondary formation of PM_{2.5} in northern China (Zhang et al.,
381 2022; Zhang et al., 2021b)(Zhang et al., 2022; Zhang et al., 2021b).

382



383

384

385

386

387

388

Figure 4. The composite anomalies of geopotential height (units: gpm) and wind vector at 500 hPa for three days for Type I and Type II, with the anomaly relative to the winter average in winter 2014-2019.

389

3.4 Pollution days in SWLY attributable to atmospheric stagnation

390

391

392

393

394

Stagnant meteorological conditions have been found to play an important role in promoting the accumulation of PM_{2.5} on severe pollution days in China (Wang et al., 2022; Wang et al., 2018a)(Wang et al., 2022; Wang et al., 2018a). Therefore, besides in addition to the days categorized as a seesaw pattern in wintertime during 2014-2019, we investigate the impact of atmospheric stagnation on PM_{2.5} pollution in SWLY.

395

396

397

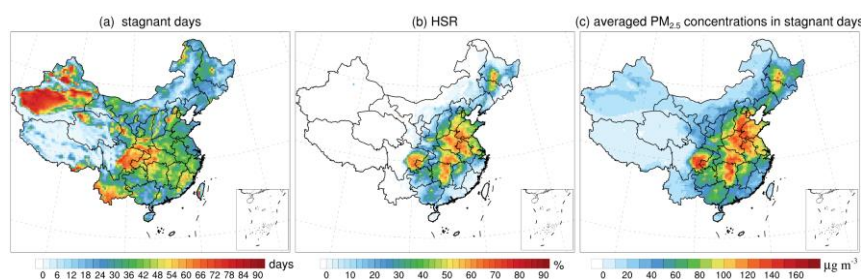
398

399

400

The annual mean of atmospheric stagnation days in 2014-2019 over eastern China is shown in Fig. 5a. The Tarim Basin and Sichuan Basin exhibit the most frequent stagnation occurrence exceeding 50%, which is attributable to the topography as well as climate conditions featured by low wind speed (Huang et al., 2017; Wang et al., 2022)(Huang et al., 2017; Wang et al., 2022). While in SWLY (green square in Fig. 1a), the annual mean stagnation days reaches 37 days. Furthermore, we evaluate

401 the capability of stagnation days to modulate PM_{2.5} pollution and use the ratio of
402 polluted days in stagnation days to the total number of stagnation days (HSR, defined
403 in [Gao et al. \(2020\)](#)~~Gao et al. (2020)~~). As shown in Fig. 5b, among all the stagnation
404 days, the pollution days in SWLY account for 60%, which can explain 35% of the total
405 pollution days (Table S3), implying the importance of stagnant weather on the
406 accumulation of PM_{2.5}. Under ~~the~~ stagnant ~~condition~~~~conditions~~, the spatial distribution
407 of ~~the~~ average PM_{2.5} concentration (Fig. 5c) shows explicit spatial heterogeneity ~~that~~
408 ~~and~~ a high PM_{2.5} concentration is captured in SWLY (120.5 $\mu\text{g m}^{-3}$).

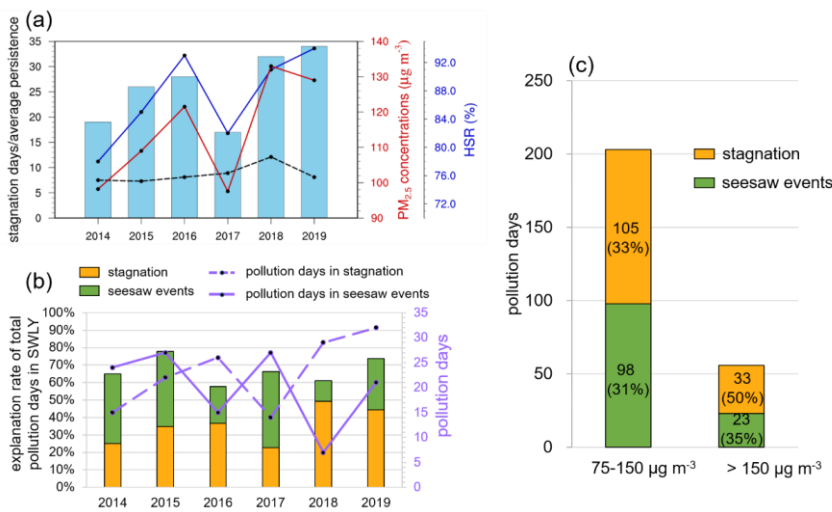


409
410 Figure 5. The annual total number of stagnant days (a), ratio of ~~the~~ pollution days to the
411 total number of stagnant days (HSR, b) and mean PM_{2.5} concentrations during stagnant
412 days during winter 2014-2019.

413
414 Furthermore, the interannual variability of ~~winter total stagnation days~~ composited
415 mean PM_{2.5} concentrations ~~and HSR~~ during stagnation ~~and HSR~~ are displayed in Fig.
416 6a, indicating consistently positive trends for the three metrics. The variability of HSR
417 and composited mean PM_{2.5} concentrations are likely governed by the variability of
418 stagnation persistence (depicted as the black dotted line in Fig. 6a). When focusing
419 specifically on pollution days (defined as daily mean PM_{2.5} concentration exceeding 75
420 $\mu\text{g m}^{-3}$) only during atmospheric stagnation, which is equivalent to the product of
421 stagnation days and HSR, yielding on average of 23 days per winter and accounting for
422 23%-49% (orange bars in Fig. 6b) of total pollution days during the winter of 2014-
423 2019. Moreover, the total number of pollution days amounts to 387 (Table S3). The
424 pollution days associated with seesaw events are laid out in green bars and account for

425 a range of 12% to 44%, with the highest proportion of 44% in 2017, following followed
 426 by 43% in 2015 and 40% in 2014, tightly linked to the interannual variability of large-
 427 scale cold fronts activities (Zhang et al., 2019c)(Zhang et al., 2019c). Overall, the
 428 stagnation of air conditions and transport account accounted for 58%-78%, on average
 429 of 67%, of the pollution days in SWLY in winter 2014-2019.

430 The pollution days can be classified into moderate pollution days ($75 \mu\text{g m}^{-3} <$
 431 $\text{PM}_{2.5} \leq 150 \mu\text{g m}^{-3}$) and heavy pollution days ($150 \mu\text{g m}^{-3} < \text{PM}_{2.5}$). For moderate
 432 pollution days, comparable contribution contributions from stagnation (33%) and
 433 seesaw events (31%) is are achieved. The contribution to the heavy pollution is even
 434 higher, accounting for 85%, with 50% from stagnation and 35% from seesaw events.

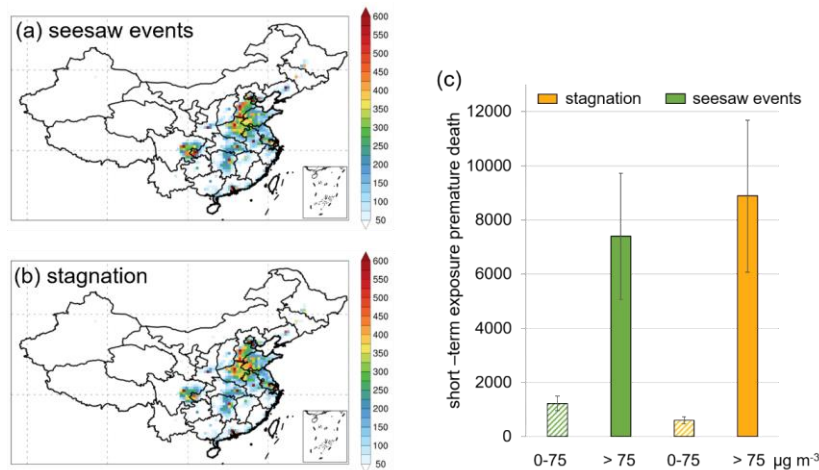


435
 436 Figure 6. (a) annualAnnual stagnation days in winter (blue bars), the average
 437 concentration of PM_{2.5} during the stagnation period (red line), HSR (the ratio of haze
 438 days during the stagnation period to the total number of stagnation days; blue line) and
 439 the average persistence of composite stagnation events in SWLY (black dotted line) in
 440 winter from 2014-2019. (b) theThe annual explanation rate of stagnant air conditions
 441 and seesaw events on total pollution days (PM_{2.5} concentrations greater than 75 μg m⁻³
 442 ³) in SWLY. (c) theThe total explanation rate of air stagnation and seesaw events on
 443 moderate pollution (75-150 μg m⁻³) and heavy pollution (>150 μg m⁻³) days in SWLY.

3.5 Premature deaths attributable to short-term PM_{2.5} exposure over SWLY

445 Considering the threat of exposure to PM_{2.5} to public health, we ~~have conducted~~
446 ~~an assessment of~~ assessed premature deaths in SWLY due to short-term PM_{2.5} exposure
447 caused by ~~the~~ seesaw events and stagnant meteorology in winter during 2014-2019.

448 There ~~is~~ was a total of 26,241 (95% CI: 18,304-34,126) premature deaths resulting
449 from PM_{2.5} exposure in SWLY in winter during 2014-2019. Specifically, during the
450 seesaw events ~~as~~ shown in Fig. 7a, focusing on ~~the~~ eastern China, the distribution of
451 premature deaths due to short-term PM_{2.5} exposure ~~is~~ mainly ~~concentrate~~ concentrated
452 in ~~the~~ southern NCP, SWLY and YRD. For SWLY, ~~the~~ PM_{2.5} exposure during the
453 seesaw events ~~accounts~~ accounted for 33% (8,634 (95% CI: 6,023-11,223)) of the total
454 premature deaths, primarily due to ~~the~~ exposure to pollution days (7,404 (95% CI:
455 5,060-9,727)) compared to clean days (green bars in Fig. 7c). A comparable premature
456 death is caused by stagnation (9,496 (95% CI: 6,552-12,413); Fig. 7b) in SWLY mainly
457 attributable to PM_{2.5} exposure ~~in~~ on pollution days (8,892 (95% CI: 6,078-11,678);
458 orange ~~bars~~ bars in Fig. 7c). We also ~~calculate~~ calculated the total number of premature
459 deaths in China during winter from 2014 to 2019 due to short-term exposure, which
460 ~~amount~~ amounted to 293,652 (95% CI: 229,711-357,318). Notably, SWLY
461 ~~account~~ accounted for 9% of these premature deaths, despite its coverage representing
462 only 0.8% of the total land area.



464
 465 Figure 7. (a) The spatial distribution of total premature deaths resulting from short-term
 466 PM_{2.5} exposure during the transport days (i.e., days with seesaw events); (b) Same as
 467 (a) but for the days with stagnation conditions in SWLY; (c) The premature deaths
 468 resulting from exposure to PM_{2.5} ~~which with~~ concentrations ~~is~~ less than 75 μg m⁻³ and
 469 greater than 75 μg m⁻³ during transport and stagnant days in SWLY.
 470

471 **Conclusions**

472 The SWLY region, located at the junction of the NCP and YRD, experiences a
 473 persistent and pronounced wintertime PM_{2.5} pollution situation from 2014 to 2019.
 474 Interestingly, despite comparable frequencies of pollution days between NCP and
 475 SWLY, the total number of pollution days in SWLY (57.1 days per year) is 14% higher
 476 than [that](#) in NCP. This can be attributed to the amplified influence of seesaw transport
 477 effects between NCP and YRD on PM_{2.5} levels in SWLY.

478 When there is a transition in the geopotential height anomaly at 500 hPa,
 479 particularly when it changes from positive to negative in northern China (or vice versa),
 480 it leads to a shift in pollutant transport. The northwest wind activity facilitates the
 481 transport of pollutants from [the](#) NCP to [the](#) YRD, while the southeasterly wind favors
 482 pollutant ~~transport~~transport from [the](#) YRD to [the](#) NCP, yielding high PM_{2.5} levels in
 483 SWLY. Moreover, atmospheric stagnation plays a crucial role in triggering PM_{2.5}
 484 accumulation in SWLY. For instance, during the winter period of 2014-2019, both the
 485 total number of stagnation days and mean PM_{2.5} concentration during stagnant periods

486 show positive trends, likely modulated by the persistence of stagnation. Overall, the
487 combined influence of seesaw events and stagnation ~~account~~accounts for
488 approximately two thirds of the pollution days observed in SWLY.

489 Considering the health effects during winters from 2014 to 2019 in SWLY, short-
490 term exposure to PM_{2.5} ~~is~~was found to result in ~~an~~ additional 8,634 premature deaths
491 (95% CI: 6,023-11,223) and 9,496 premature deaths (95% CI: 6,552-12,413)
492 attributable to seesaw events and stagnation, respectively. ~~Despite~~Although the
493 ~~area~~area of SWLY ~~covers~~accounts for less than 1% ~~in~~of China, ~~it accounts for 9% of~~
494 the total number of premature deaths in ~~SWLY~~ ~~accounted for 9% of~~the country. More
495 frequent atmospheric stagnation events are projected to occur in China under a warming
496 climate (~~Horton et al., 2014; Hu et al., 2022~~)(Horton et al., 2014; Hu et al., 2022),
497 highlighting the urgency of coordinated cross-regional emissions reduction to achieve
498 additional benefits in reducing PM_{2.5} concentrations and the associated health effect in
499 SWLY.

500

501 **Data availability**

502 The regional air quality simulations are available upon request to the corresponding
503 author.

504

505 **Author contributions**

506 Y.G. conceived the project, Y.F.F performed the analysis and drafted the manuscript,
507 and all authors contributed to the writing of the manuscript.

508

509 **Competing interests.** At least one of the (co-)authors is a member of the editorial board
510 of Atmospheric Chemistry and Physics.

511

512 **Acknowledgement**

513 This work was supported by the National Natural Science Foundation of China
514 (42122039) and Fundamental Research Funds for the Central Universities (202341001).

515 The simulations were conducted on the Center for High Performance Computing and
516 System Simulation, [National Laoshan Laboratory for Marine Science and Technology](#)
517 [\(Qingdao\)](#).

518

519 **References**

- 520 [Ali, M.A., Huang, Z., Bilal, M., Assiri, M.E., Mhawish, A., Nichol, J.E., et al., 2023. Long-term PM2.5](#)
521 [pollution over China: Identification of PM2.5 pollution hotspots and source contributions.](#)
522 [Science of The Total Environment. 893, 164871.](#)
- 523 Appel, K.W., Bash, J.O., Fahey, K.M., Foley, K.M., Gilliam, R.C., Hogrefe, C., et al., 2021. The
524 Community Multiscale Air Quality (CMAQ) model versions 5.3 and 5.3.1: system updates and
525 evaluation. *Geoscientific Model Development*. 14, 2867-2897.
- 526 Appel, K.W., Gilliland, A.B., Sarwar, G., Gilliam, R.C., 2007. Evaluation of the Community Multiscale
527 Air Quality (CMAQ) model version 4.5: Sensitivities impacting model performance: Part I—
528 Ozone. *Atmospheric Environment*. 41, 9603-9615.
- 529 Berman, A., Adhikari, T., Mukhopadhyay, S., Baraki, A., Tessema, Z., 2020. Global burden of 369
530 diseases and injuries in 204 countries and territories, 1990–2019: a systematic analysis for the.
- 531 [Bowden, J.H., Otte, T.L., Nolte, C.G., Otte, M.J., 2012. Examining Interior Grid Nudging Techniques](#)
532 [Using Two-Way Nesting in the WRF Model for Regional Climate Modeling. Journal of Climate.](#)
533 [25, 2805-2823.](#)
- 534 [Brioude, J., Arnold, D., Stohl, A., Cassiani, M., Morton, D., Seibert, P., et al., 2013. The Lagrangian](#)
535 [particle dispersion model FLEXPART-WRF version 3.1. Geosci. Model Dev. 6, 1889-1904.](#)
- 536 Donaldson, K., Li, X.Y., MacNee, W., 1998. Ultrafine (nanometre) particle mediated lung injury. *Journal*
537 *of Aerosol Science*. 29, 553-560.
- 538 Emery, C., Tai, E. Enhanced Meteorological Modeling and Performance Evaluation for Two Texas Ozone
539 Episodes, 2001.
- 540 Emmons, L.K., Walters, S., Hess, P.G., Lamarque, J.F., Pfister, G.G., Fillmore, D., et al., 2010.
541 Description and evaluation of the Model for Ozone and Related chemical Tracers, version 4
542 (MOZART-4). *Geoscientific Model Development*. 3, 43-67.
- 543 EPA, U. Guidance on the Use of Models and Other Analyses for Demonstrating Attainment of Air Quality
544 Goals for Ozone, PM2.5 and Regional Haze. Vol EPA -454/B-07-002, 2007.
- 545 Gao, Y., Zhang, L., Huang, A., Kou, W., Bo, X., Cai, B., et al., 2022. Unveiling the spatial and sectoral
546 characteristics of a high-resolution emission inventory of CO2 and air pollutants in China.
547 *Science of The Total Environment*. 847, 157623.
- 548 Gao, Y., Zhang, L., Zhang, G., Yan, F.F., Zhang, S.Q., Sheng, L.F., et al., 2020. The climate impact on
549 atmospheric stagnation and capability of stagnation indices in elucidating the haze events over
550 North China Plain and Northeast China. *Chemosphere*. 258, 12.
- 551 [Geng, G., Xiao, Q., Liu, S., Liu, X., Cheng, J., Zheng, Y., et al., 2021. Tracking Air Pollution in China:](#)
552 [Near Real-Time PM2.5 Retrievals from Multisource Data Fusion. Environmental Science &](#)
553 [Technology. 55, 12106-12115.](#)
- 554 Giglio, L., Randerson, J.T., van der Werf, G.R., 2013. Analysis of daily, monthly, and annual burned area
555 using the fourth-generation global fire emissions database (GFED4). *Journal of Geophysical*
556 *Research-Biogeosciences*. 118, 317-328.

557 Guenther, A.B., Jiang, X., Heald, C.L., Sakulyanontvittaya, T., Duhl, T., Emmons, L.K., et al., 2012. The
558 Model of Emissions of Gases and Aerosols from Nature version 2.1 (MEGAN2.1): an extended
559 and updated framework for modeling biogenic emissions. *Geoscientific Model Development*.
560 5, 1471-1492.

561 He, J., Gong, S., Zhou, C., Lu, S., Wu, L., Chen, Y., et al., 2018. Analyses of winter circulation types and
562 their impacts on haze pollution in Beijing. *Atmospheric Environment*. 192, 94-103.

563 Horton, D.E., Skinner, C.B., Singh, D., Diffenbaugh, N.S., 2014. Occurrence and persistence of future
564 atmospheric stagnation events. *Nature Climate Change*. 4, 698-703.

565 Hu, A., Xie, X., Gong, K., Hou, Y., Zhao, Z., Hu, J., 2022. Assessing the Impacts of Climate Change on
566 Meteorology and Air Stagnation in China Using a Dynamical Downscaling Method. *Frontiers
567 in Environmental Science*. 10.

568 Hua, W.L., Wu, B.Y., 2022. Atmospheric circulation anomaly over mid- and high-latitudes and its
569 association with severe persistent haze events in Beijing. *Atmospheric Research*. 277.

570 Huang, Q.Q., Cai, X.H., Song, Y., Zhu, T., 2017. Air stagnation in China (1985-2014): climatological
571 mean features and trends. *Atmospheric Chemistry and Physics*. 17, 7793-7805.

572 Huang, X., Ding, A.J., Wang, Z.L., Ding, K., Gao, J., Chai, F.H., et al., 2020. Amplified transboundary
573 transport of haze by aerosol-boundary layer interaction in China. *Nature Geoscience*. 13, 428-
574 +.

575 Jia, Z.X., Doherty, R.M., Ordonez, C., Li, C.F., Wild, O., Jain, S., et al., 2022. The impact of large-scale
576 circulation on daily fine particulate matter (PM_{2.5}) over major populated regions of China in
577 winter. *Atmospheric Chemistry and Physics*. 22, 6471-6487.

578 Jiang, Z., Jolleys, M.D., Fu, T.-M., Palmer, P.I., Ma, Y., Tian, H., et al., 2020. Spatiotemporal and
579 probability variations of surface PM_{2.5} over China between 2013 and 2019 and the associated
580 changes in health risks: An integrative observation and model analysis. *Science of The Total
581 Environment*. 723, 137896.

582 Kang, H.Q., Zhu, B., Gao, J.H., He, Y., Wang, H.L., Su, J.F., et al., 2019. Potential impacts of cold frontal
583 passage on air quality over the Yangtze River Delta, China. *Atmospheric Chemistry and Physics*.
584 19, 3673-3685.

585 Kang, H.Q., Zhu, B., Liu, X.H., Shi, S.S., Hou, X.W., Lu, W., et al., 2021. Three-Dimensional
586 Distribution of PM_{2.5} over the Yangtze River Delta as Cold Fronts Moving Through. *Journal
587 of Geophysical Research-Atmospheres*. 126, 11.

588 Li, J.D., Liao, H., Hu, J.L., Li, N., 2019a. Severe particulate pollution days in China during 2013-2018
589 and the associated typical weather patterns in Beijing-Tianjin-Hebei and the Yangtze River
590 Delta regions. *Environmental Pollution*. 248, 74-81.

591 Li, M., Liu, H., Geng, G.N., Hong, C.P., Liu, F., Song, Y., et al., 2017. Anthropogenic emission
592 inventories in China: a review. *National Science Review*. 4, 834-866.

593 Li, T.T., Guo, Y.M., Liu, Y., Wang, J.N., Wang, Q., Sun, Z.Y., et al., 2019b. Estimating mortality burden
594 attributable to short-term PM_{2.5} exposure: A national observational study in China.
595 *Environment International*. 125, 245-251.

596 Liu, C., Chen, R., Sera, F., Vicedo-Cabrera, A.M., Guo, Y., Tong, S., et al., 2019a. Ambient Particulate
597 Air Pollution and Daily Mortality in 652 Cities. *New England Journal of Medicine*. 381, 705-
598 715.

599 Liu, H., Fu, M.L., Jin, X.X., Shang, Y., Shindell, D., Faluvegi, G., et al., 2016. Health and climate impacts
600 of ocean-going vessels in East Asia. *Nature Climate Change*. 6, 1037-+.

-
- 601 Liu, H., Meng, Z.H., Lv, Z.F., Wang, X.T., Deng, F.Y., Liu, Y., et al., 2019b. Emissions and health impacts
602 from global shipping embodied in US-China bilateral trade. *Nature Sustainability*. 2, 1027-1033.
- 603 Liu, J., Yin, H., Tang, X., Zhu, T., Zhang, Q., Liu, Z., et al., 2021. Transition in air pollution, disease
604 burden and health cost in China: A comparative study of long-term and short-term exposure.
605 *Environmental Pollution*. 277.
- 606 [Liu, P., Tsimpidi, A.P., Hu, Y., Stone, B., Russell, A.G., Nenes, A., 2012. Differences between
607 downscaling with spectral and grid nudging using WRF. *Atmos. Chem. Phys.* 12, 3601-3610.](#)
- 608 Luecken, D.J., Yarwood, G., Hutzell, W.T., 2019. Multipollutant modeling of ozone, reactive nitrogen
609 and HAPs across the continental US with CMAQ-CB6. *Atmospheric Environment*. 201, 62-72.
- 610 Ma, M.C., Gao, Y., Wang, Y.H., Zhang, S.Q., Leung, L.R., Liu, C., et al., 2019. Substantial ozone
611 enhancement over the North China Plain from increased biogenic emissions due to heat waves
612 and land cover in summer 2017. *Atmospheric Chemistry and Physics*. 19, 12195-12207.
- 613 Ma, Q.X., Wu, Y.F., Zhang, D.Z., Wang, X.J., Xia, Y.J., Liu, X.Y., et al., 2017. Roles of regional transport
614 and heterogeneous reactions in the PM_{2.5} increase during winter haze episodes in Beijing.
615 *Science of the Total Environment*. 599, 246-253.
- 616 MEEPRC. Technical regulation on ambient air quality index (on trial): HJ 633. 2022, 2012.
- 617 Pui, D.Y.H., Chen, S.C., Zuo, Z.L., 2014. PM_{2.5} in China: Measurements, sources, visibility and health
618 effects, and mitigation. *Particuology*. 13, 1-26.
- 619 Pye, H.O.T., Murphy, B.N., Xu, L., Ng, N.L., Carlton, A.G., Guo, H.Y., et al., 2017. On the implications
620 of aerosol liquid water and phase separation for organic aerosol mass. *Atmospheric Chemistry
621 and Physics*. 17, 343-369.
- 622 Saha, S., Moorthi, S., Wu, X.R., Wang, J., Nadiga, S., Tripp, P., et al., 2014. The NCEP Climate Forecast
623 System Version 2. *Journal of Climate*. 27, 2185-2208.
- 624 Sun, Y., Zhang, Y., Chen, C., Sun, Q., Wang, Y., Du, H., et al., 2022. Impact of Heavy PM_{2.5} Pollution
625 Events on Mortality in 250 Chinese Counties. *Environmental Science & Technology*. 56, 8299-
626 8307.
- 627 Van der Werf, G.R., Randerson, J.T., Giglio, L., van Leeuwen, T.T., Chen, Y., Rogers, B.M., et al., 2017.
628 Global fire emissions estimates during 1997-2016. *Earth System Science Data*. 9, 697-720.
- 629 Wang, J., Liu, Y., Ding, Y., Wu, P., Zhu, Z., Xu, Y., et al., 2020. Impacts of climate anomalies on the
630 interannual and interdecadal variability of autumn and winter haze in North China: A review.
631 *International Journal of Climatology*. 40, 4309-4325.
- 632 Wang, L.H., Newchurch, M.J., Biazar, A., Liu, X., Kuang, S., Khan, M., et al., 2011. Evaluating
633 AURA/OMI ozone profiles using ozonesonde data and EPA surface measurements for August
634 2006. *Atmospheric Environment*. 45, 5523-5530.
- 635 Wang, L.L., Li, M.G., Wang, Q.L., Li, Y.Y., Xin, J.Y., Tang, X., et al., 2022. Air stagnation in China:
636 Spatiotemporal variability and differing impact on PM_{2.5} and O₃ during 2013-2018. *Science
637 of the Total Environment*. 819.
- 638 Wang, X.Y., Dickinson, R.E., Su, L.Y., Zhou, C.L.E., Wang, K.C., 2018a. PM_{2.5} POLLUTION IN
639 CHINA AND HOW IT HAS BEEN EXACERBATED BY TERRAIN AND
640 METEOROLOGICAL CONDITIONS. *Bulletin of the American Meteorological Society*. 99,
641 105-120.
- 642 Wang, X.Y., Dickinson, R.E., Su, L.Y., Zhou, C.L.E., Wang, K.C., 2018b. PM_{2.5} pollution in China and
643 how it has been exacerbated by terrain and meteorological conditons. *Bulletin of the American
644 Meteorological Society*. 99, 105-120.

645 Wang, Y.S., Yao, L., Wang, L.L., Liu, Z.R., Ji, D.S., Tang, G.Q., et al., 2014. Mechanism for the formation
646 of the January 2013 heavy haze pollution episode over central and eastern China. *Science China-*
647 *Earth Sciences*. 57, 14-25.

648 Wu, X.G., Ding, Y.Y., Zhou, S.B., Tan, Y., 2018. Temporal characteristic and source analysis of PM2.5
649 in the most polluted city agglomeration of China. *Atmospheric Pollution Research*. 9, 1221-
650 1230.

651 Xie, Y., Dai, H.C., Dong, H.J., Hanaoka, T., Masui, T., 2016. Economic Impacts from PM2.5 Pollution-
652 Related Health Effects in China: A Provincial-Level Analysis. *Environmental Science &*
653 *Technology*. 50, 4836-4843.

654 Xing, Y.F., Xu, Y.H., Shi, M.H., Lian, Y.X., 2016. The impact of PM2.5 on the human respiratory system.
655 *Journal of Thoracic Disease*. 8, E69-E74.

656 Yang, Y., Luo, L.W., Song, C., Yin, H., Yang, J.T., 2018. Spatiotemporal Assessment of PM2.5-Related
657 Economic Losses from Health Impacts during 2014-2016 in China. *International Journal of*
658 *Environmental Research and Public Health*. 15.

659 Zeng, X.R., Gao, Y., Wang, Y.H., Ma, M.C., Zhang, J.X., Sheng, L.F., 2022. Characterizing the distinct
660 modulation of future emissions on summer ozone concentrations between urban and rural areas
661 over China. *Science of the Total Environment*. 820, 11.

662 Zhang, G., Gao, Y., Cai, W., Leung, L.R., Wang, S., Zhao, B., et al., 2019a. Seesaw haze pollution in
663 North China modulated by the sub-seasonal variability of atmospheric circulation. *Atmos.*
664 *Chem. Phys.* 19, 565-576.

665 Zhang, J., Yuan, Q., Liu, L., Wang, Y.Y., Zhang, Y.X., Xu, L., et al., 2021a. Trans-Regional Transport of
666 Haze Particles From the North China Plain to Yangtze River Delta During Winter. *Journal of*
667 *Geophysical Research-Atmospheres*. 126.

668 Zhang, Q., Quan, J.N., Tie, X.X., Li, X., Liu, Q., Gao, Y., et al., 2015. Effects of meteorology and
669 secondary particle formation on visibility during heavy haze events in Beijing, China. *Science*
670 *of the Total Environment*. 502, 578-584.

671 Zhang, Q., Zheng, Y.X., Tong, D., Shao, M., Wang, S.X., Zhang, Y.H., et al., 2019b. Drivers of improved
672 PM2.5 air quality in China from 2013 to 2017. *Proceedings of the National Academy of*
673 *Sciences of the United States of America*. 116, 24463-24469.

674 Zhang, S., Zeng, G., Wang, T., Yang, X., Iyakaremye, V., 2022. Three dominant synoptic atmospheric
675 circulation patterns influencing severe winter haze in eastern China. *Atmos. Chem. Phys.* 22,
676 16017-16030.

677 Zhang, W., Hai, S., Zhao, Y., Sheng, L., Zhou, Y., Wang, W., et al., 2021b. Numerical modeling of
678 regional transport of PM2.5 during a severe pollution event in the Beijing–Tianjin–Hebei region
679 in November 2015. *Atmospheric Environment*. 254, 118393.

680 Zhang, X., Xu, X., Ding, Y., Liu, Y., Zhang, H., Wang, Y., et al., 2019c. The impact of meteorological
681 changes from 2013 to 2017 on PM2.5 mass reduction in key regions in China. *Science China*
682 *Earth Sciences*. 62, 1885-1902.

683 Zheng, B., Tong, D., Li, M., Liu, F., Hong, C.P., Geng, G.N., et al., 2018. Trends in China's anthropogenic
684 emissions since 2010 as the consequence of clean air actions. *Atmospheric Chemistry and*
685 *Physics*. 18, 14095-14111.

686 Zhong, W., Yin, Z., Wang, H., 2019. The relationship between anticyclonic anomalies in northeastern
687 Asia and severe haze in the Beijing–Tianjin–Hebei region. *Atmos. Chem. Phys.* 19, 5941-5957.

688